Prioritize Alignment in Dataset Distillation

Zekai Li[1][*], **Ziyao Guo**[1][*], **Wangbo Zhao**[1], **Tianle Zhang**[1], **Zhi-Qi Cheng**[2], **Samir Khaki**[3],
Kaipeng Zhang[4], **Ahmad Sajedi**[3], **Konstantinos N Plataniotis**[3], **Kai Wang**[1][†], **Yang You**[1]
[1]National University of Singapore [2]Carnegie Mellon University
[3]University of Toronto [4]Shanghai AI Laboratory
Code: NUS-HPC-AI-Lab/PAD

Abstract

Dataset Distillation aims to compress a large dataset into a significantly more compact, synthetic one without compromising the performance of the trained models. To achieve this, existing methods use the agent model to extract information from the target dataset and embed it into the distilled dataset. Consequently, the quality of extracted and embedded information determines the quality of the distilled dataset. In this work, we find that existing methods introduce misaligned information in both information extraction and embedding stages. To alleviate this, we propose Prioritize Alignment in Dataset Distillation (**PAD**), which aligns information from the following two perspectives. 1) We prune the target dataset according to the compressing ratio to filter the information that can be extracted by the agent model. 2) We use only deep layers of the agent model to perform the distillation to avoid excessively introducing low-level information. This simple strategy effectively filters out misaligned information and brings non-trivial improvement for mainstream matching-based distillation algorithms. Furthermore, built on trajectory matching, **PAD** achieves remarkable improvements on various benchmarks, achieving state-of-the-art performance.

1 Introduction

Dataset Distillation (DD) [47] aims to compress a large dataset into a small synthetic dataset that preserves important features for models to achieve comparable performances. Ever since being introduced, DD has gained a lot of attention because of its wide applications in practical fields such as privacy preservation [6, 50], continual learning [30, 37], and neural architecture search [13, 34].

Recently, matching-based methods [7, 46, 52] have achieved promising performance in distilling high-quality synthetic datasets. Generally, the process of these methods can be summarized into two steps: (1) *Information Extraction*: an agent model is used to extract important information from the target dataset by recording various metrics such as gradients [55], distributions [54], and training trajectories [1], (2) *Information Embedding*: the synthetic samples are optimized to incorporate the extracted information, which is achieved by minimizing the differences between the same metric calculated on the synthetic data and the one recorded in the previous step.

In this work, we first reveal both steps will introduce misaligned information, which is redundant and potentially detrimental to the quality of the synthetic data. Then, by analyzing the cause of this misalignment, we propose alleviating this problem through the following two perspectives.

Typically, in the *Information Extraction* step, most distillation methods allow the agent model to see all samples in the target dataset. This means information extracted by the agent model comes

---

[*]equal contribution, {lizekai, ziyao}@u.nus.edu

[†]corresponding author, kai.wang@comp.nus.edu.sg

(a) Data used for distillation
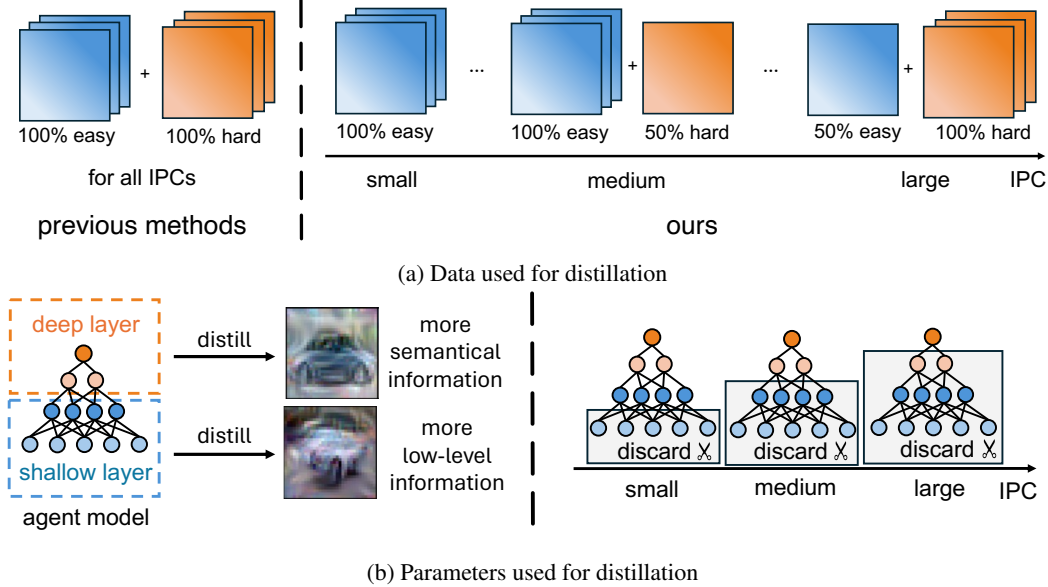

(b) Parameters used for distillation

Figure 1: (a) Compared with using all samples without differentiation in IPCs (left), PAD meticulously selects a subset of samples for different IPCs to align the expected difficulty of information required (right). (b) Different layers distill different patterns (left). PAD masks out (grey box) shallow-layer parameters during metric matching in accordance with IPCs (right).

from samples with various difficulties (see Figure 1(a)). However, according to previous study [11], information related to easy samples is only needed when the compression ratio is high. This misalignment leads to the sub-optimal of the distillation performance.

To alleviate the above issue, we first use data selection methods to measure the difficulty of each sample in the target dataset. Then, during the distillation, a data scheduler is employed to ensure only data whose difficulty is aligned with the compression ratio is available for the agent model.

In the *Information Embedding* step, most distillation methods except DM [54] choose to use all parameters of the agent model to perform the distillation. Intuitively, this will ensure the information extracted by the agent model is fully utilized. However, we find shallow layer parameters of the model can only provide low-quality, basic signals, which are redundant for dataset distillation in most cases. Conversely, performing the distillation with only parameters from deep layers will yield high-quality synthetic samples. We attribute this contradiction to the fact that deeper layers in DNNs tend to learn higher-level representations of input data [29, 39].

Based on our findings, to avoid embedding misaligned information in the *Information Embedding* step, we propose to use only parameters from deeper layers of the agent model to perform distillation, as illustrated in Figure 1(b). This simple change brings significant performance improvement, showing its effectiveness in aligning information.

Through experiments, we validate that our two-step alignment strategy is effective for distillation methods based on matching gradients [55], distributions [54], and trajectories [1]. Moreover, by applying our alignment strategy on trajectory matching [1, 11], we propose our novel method named Prioritize Alignment in Dataset Distillation (PAD). After conducting comprehensive evaluation experiments, we show PAD achieves state-of-the-art (SOTA) performance.

2   Misaligned Information in Dataset Distillation

Generally, we can summarize the distillation process of matching-based methods into the following two steps: (1) *Information Extraction*: use an agent model to extract essential information from the target dataset, realized by recording metrics such as gradients [55], distributions [54], and training trajectories [1], (2) *Information Embedding*: the synthetic samples are optimized to incorporate the extracted information, realized by minimizing the differences between the same metric calculated on the synthetic data and the one recorded in the first step.
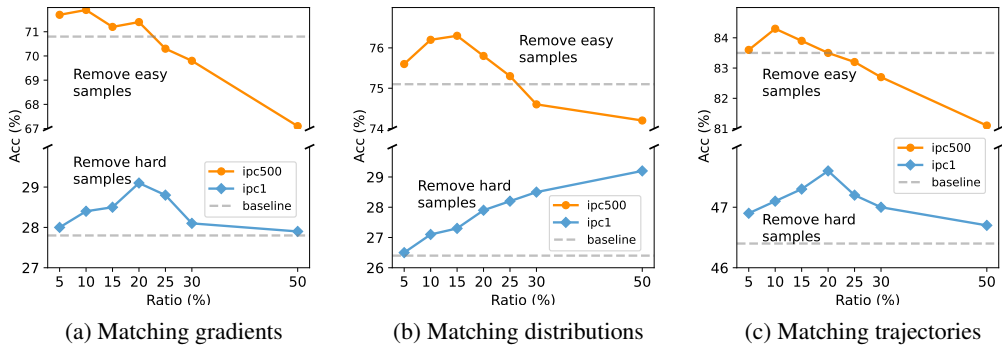
Figure 2: Distillation performance on CIFAR-10 where data points are removed with different ratios. Removing unnecessary data points helps to improve the performance of methods based on matching gradients, distributions, and trajectories, both in low and high IPC cases.
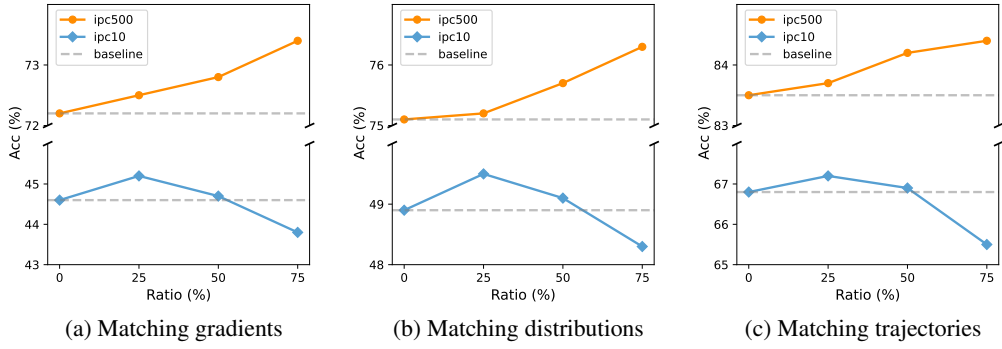

Figure 3: Distillation performances on CIFAR-10 where n% (ratio) shallow layer parameters are not utilized during distillation. Discarding shallow-layer parameters is beneficial for methods based on matching gradients, distributions, and trajectories, both in low and high IPC cases.

In this section, through analyses and experimental verification, we show the above two steps both will introduce misaligned information to the synthetic data.

2.1 Misaligned Information Extracted by Agent Models

In the *information extraction* step, an agent model is employed to extract information from the target dataset. Generally, most existing methods [1, 7, 52, 55] allow the agent model to see the full dataset. This implies that the information extracted by the agent model originates from samples with diverse levels of difficulty. However, the expected difficulty of distilled information varies with changes in IPC: smaller IPCs prefer easier information while larger IPCs should distill harder one [11].

To verify if this misalignment will influence the quality of synthetic data, we perform the distillation where hard/easy samples of target dataset are removed with various ratios. As the results reported in Figure 2, pruning unaligned data points is beneficial for all matching-based methods. This proves the misalignment indeed will influence the distillation performance and can be alleviated by filtering out misaligned data from the target dataset.

2.2 Misaligned Information Embedded by Metric Matching

Most existing methods use all parameters of the agent model to compute the metric used for matching. Intuitively, this helps to improve the distillation performance, since in this way all information extracted by the agent model will be embedded into the synthetic dataset. However, since shallow layers in DNNs tend to learn basic distributions of data [29, 39], using parameters from these layers can only provide low-level signals that turned out to be redundant in most cases.

3

As can be observed in Figure 3, it is evident that across all matching-based methods, the removal of shallow layer parameters consistently enhances performance, regardless of the IPC setting. This proves employing over-shallow layer parameters to perform the distillation will introduce misaligned information to the synthetic data, compromising the quality of distilled data.

3   Method

To alleviate the information misalignment issue, based on trajectory matching (TM) [1, 11], we propose Prioritizing Alignment in Dataset Distillation (PAD). PAD can also be applied to methods based on matching gradients [55] and distributions [54], which are introduced in Appendix **??**.

3.1   Preliminary of Trajectory Matching

Following the two-step procedure, to extract information, TM-based methods [1, 11] first train agent models on the real dataset $\mathcal{D}_R$ and record the changes of the parameters. Specifically, let $\{\theta_t^*\}_0^N$ be an expert trajectory, which is a parameter sequence recorded during the training of agent model. At each iteration of trajectory matching, θ_t^* and θ_{t+M}^* are randomly selected from expert trajectories as the start and target parameters.

To embed the information into the synthetic data, TM methods minimize the distance between the expert trajectory and the student trajectory. Let $\hat{\theta}_t$ denote the parameters of the student agent model trained on synthetic dataset $\mathcal{D}_S$ at timestep t. The student trajectory progresses by doing gradient descent on the cross-entropy loss l for N steps:

$$\hat{\theta}_{t+i+1} = \hat{\theta}_{t+i} - \alpha \nabla l(\hat{\theta}_{t+i}, \mathcal{D}_S), \tag{1}$$

Finally, the synthetic data is optimized by minimizing the distance metric, which is formulated as:

$$\mathcal{L} = \frac{||\hat{\theta}_{t+N} - \theta_{t+M}^*||}{||\theta_{t+M}^* - \theta_t^*||}. \tag{2}$$

3.2   Filtering Information Extraction

In section 2.1, we show using data selection to filter out unmatched samples could alleviate the misalignment caused in *Information Extraction* step. According to previous work [11], TM-based methods prefer easy information and choose to match only early trajectories when IPC is small. Conversely, hard information is preferred by high IPCs and they match only late trajectories. Hence, we should use easy samples to train early trajectories, while late trajectories should be trained with hard samples. To realize this efficiently, we first use the data selection method to measure the difficulty of samples contained in the target dataset. Then, during training expert trajectories, a scheduler is implemented to gradually incorporate hard samples into the training set while excluding easier ones.

Difficulty Scoring Function   Identifying the difficulty of data for DNNs to learn has been well studied in data selection area [17, 18, 31, 42]. For simplicity consideration, we use Error L2-Norm (EL2N) score [35] as the metric to evaluate the difficulty of training examples (other metrics can also be chosen, see Section 4.3.2). Specifically, let x and y denote a data point and its label, respectively. Then, the EL2N score can be calculated by:

$$\chi_t(x, y) = \mathbb{E}||p(w_t, x) - y||_2. \tag{3}$$

where $p(w_t, x) = \sigma(f(w_t, x))$ is the output of a model f at training step t transformed into a probability distribution. In consistent with [42], samples with higher EL2N scores are considered as harder samples in this paper.

Scheduler   The scheduler can be divided into the following stages. Firstly, the hardest samples are removed from the training set, ensuring that it exclusively comprises data meeting a predetermined initial ratio (IR). Then, during training expert trajectories, samples are gradually added to the training set in order of increasing difficulty. After incorporating all the data into the training set, the scheduler will begin to remove easy samples from the target dataset. Unlike the gradual progression involved in adding data, the action of reducing data is completed in a single operation, since now the model has been trained on simple samples for a sufficient time. (Please refer to Appendix A.2 for experimental comparisons)

Dataset	CIFAR-10					CIFAR-100				Tiny ImageNet		
IPC	1	10	50	500	1000	1	10	50	100	1	10	50
Ratio	0.02	0.2	1	10	20	0.2	2	10	20	0.2	2	10
Random	15.4±0.3	31.0±0.5	50.6±0.3	73.2±0.3	78.4±0.2	4.2±0.3	14.6±0.5	33.4±0.4	42.8±0.3	1.4±0.1	5.0±0.2	15.0±0.4
KIP [33]	49.9±0.2	62.7±0.3	68.6±0.2	-	-	15.7±0.2	28.3±0.1	-	-	-	-	-
FRePo [56]	46.8±0.7	65.5±0.4	71.7±0.2	-	-	28.7±0.1	42.5±0.2	44.3±0.2	-	15.4±0.3	25.4±0.2	-
RCIG [28]	53.9±1.0	69.1±0.4	73.5±0.3	-	-	39.3±0.4	44.1±0.4	46.7±0.3	-	25.6±0.3	29.4±0.2	-
DC [55]	28.3±0.5	44.9±0.5	53.9±0.5	72.1±0.4	76.6±0.3	12.8±0.3	25.2±0.3	-	-	-	-	-
DM [54]	26.0±0.8	48.9±0.6	63.0±0.4	75.1±0.3	78.8±0.1	11.4±0.3	29.7±0.3	43.6±0.4	-	3.9±0.2	12.9±0.4	24.1±0.3
DSA [53]	28.8±0.7	52.1±0.5	60.6±0.5	73.6±0.3	78.7±0.3	13.9±0.3	32.3±0.3	42.8±0.4	-	-	-	-
TESLA [5]	**48.5±0.8**	66.4±0.8	72.6±0.7	-	-	24.8±0.4	41.7±0.3	47.9±0.3	49.2±0.4	-	-	-
CAFE [46]	30.3±1.1	46.3±0.6	55.5±0.6	-	-	12.9±0.3	27.8±0.3	37.9±0.3	-	-	-	-
MTT [1]	46.2±0.8	65.4±0.7	71.6±0.2	-	-	24.3±0.3	39.7±0.4	47.7±0.2	49.2±0.4	8.8±0.3	23.2±0.2	28.0±0.3
FTD [7]	46.0±0.4	65.3±0.4	73.2±0.2	-	-	24.4±0.4	42.5±0.2	48.5±0.3	49.7±0.4	10.5±0.2	23.4±0.3	28.2±0.4
ATT [25]	48.3±1.0	67.7±0.6	74.5±0.4	-	-	26.1±0.3	44.2±0.5	51.2±0.3	-	11.0±0.5	25.8±0.4	-
DATM [11]	46.9±0.5	66.8±0.2	76.1±0.3	83.5±0.2	85.5±0.4	27.9±0.2	47.2±0.4	55.0±0.2	57.5±0.2	17.1±0.3	31.1±0.3	39.7±0.3
PAD	47.2±0.6	**67.4±0.3**	**77.0±0.5**	**84.6±0.3**	**86.7±0.2**	**28.4±0.5**	**47.8±0.2**	**55.9±0.3**	**58.5±0.3**	**17.7±0.2**	**32.3±0.4**	**41.6±0.4**
Full Dataset	84.8±0.1					56.2±0.3				37.6±0.4		

Table 1: Comparison with previous dataset distillation methods (bottom: matching-based, top: others) on CIFAR-10, CIFAR-100 and Tiny ImageNet. ConvNet is used for the distillation and evaluation. Our method consistently outperforms prior matching-based methods.

3.3 Filtering Information Embedding

To filter out misaligned information introduced by matching shallow-layer parameters, we propose to add a parameter selection module that masks out part of shallow layers for metric computation. Specifically, parameters of an agent network can be represented as a flattened array of length L that stores weights of agent models ordered from shallow to deep layers (parameters within the same layer are sorted in default order). The parameter selection sets a threshold ratio α such that the first $k = L \cdot \alpha$ parameters are not used for distillation. Then the parameters used for matching can now be formulated as:

$$\hat{\theta}_{t+N} = \{\underbrace{\hat{\theta}_0, \hat{\theta}_1, \cdots, \hat{\theta}_{k-1}}_{\text{discard}}, \underbrace{\hat{\theta}_k, \hat{\theta}_{k+1}, \cdots, \hat{\theta}_L}_{\text{used for matching}}\}. \tag{4}$$

In practice, the ratio α should vary with the change of IPC. For smaller IPCs, it is necessary to incorporate basic information thus α should be lower. Conversely, basic information is redundant in larger IPC cases, so α should be higher accordingly.

4 Experiments

4.1 Settings

We compare PAD with several prominent dataset distillation methods, which can be divided into two categories: matching-based approaches including DC [55], DM [54], DSA [53], CAFE [46], MTT [1], FTD [7], DATM [11], TESLA [5], and kernel-based approaches including KIP [33], FRePo [56], RCIG [28]. The assessment is conducted on widely recognized datasets: CIFAR-10, CIFAR-100[19], and Tiny ImageNet [21]. We implemented our method based on DATM [11]. In both the distillation and evaluation phases, we apply the standard set of differentiable augmentations commonly used in previous studies [1, 7, 11]. By default, networks are constructed with instance normalization unless explicitly labeled with "-BN," indicating batch normalization (e.g., ConvNet-BN). For CIFAR-10 and CIFAR-100, distillation is typically performed using a 3-layer ConvNet, while Tiny ImageNet requires a 4-layer ConvNet. Cross-architecture experiments also utilize LeNet [22], AlexNet [20], VGG11 [41], and ResNet18 [12]. More details can be found in the appendix.

4.2 Main Results

CIFAR and Tiny ImageNet We conduct comprehensive experiments to compare the performance of our method with previous works. As the results presented in Table 1, PAD outperforms previous matching-based methods on three datasets except for the case when IPC=1. When compared with kernel-based methods, which use a larger network to perform the distillation, our technique exhibits superior performance in most cases, particularly when the compression ratio exceeds 1%. As can be observed, PAD performs relatively better when IPC is high, enabling the setting of IPC500 on CIFAR-10 to also achieve lossless performance. This suggests that our filtering out misaligned

Dataset	Ratio	Method	ConvNet	ConvNet-BN	ResNet18	ResNet18-BN	VGG11	AlexNet	LeNet	MLP	Avg.
CIFAR-10	20%	Random	78.38	80.25	84.58	87.21	80.81	80.75	61.85	50.98	75.60
		Glister	62.46	70.52	81.10	74.59	78.07	70.55	56.56	40.59	66.81
		Forgetting	76.27	80.06	85.67	87.18	82.04	81.35	64.59	52.21	76.17
		DATM	85.50	85.23	**87.22**	**88.13**	**84.65**	85.14	66.70	52.40	79.37
		PAD	**86.90**	**85.67**	86.95	88.09	84.34	**85.83**	**67.28**	**53.62**	**79.84**
		↑	+8.52	+5.42	+2.37	+0.88	+3.53	+5.08	+5.43	+2.64	+4.24
CIFAR-100	20%	Random	42.80	46.38	47.48	55.62	42.69	38.05	25.91	20.66	39.95
		Glister	35.45	37.13	42.49	46.14	43.06	28.58	23.33	17.08	34.16
		Forgetting	45.52	49.99	51.44	54.65	43.28	43.47	27.22	22.90	42.30
		DATM	57.50	57.75	57.98	**63.34**	**55.10**	55.69	33.57	26.39	50.92
		PAD	**58.50**	**58.66**	**58.15**	63.17	55.02	**55.93**	**33.87**	**27.12**	**51.30**
		↑	+15.70	+12.28	+10.67	+7.55	+12.33	+17.88	+7.96	+6.46	+11.35
Tiny-ImageNet	10%	Random	15.00	24.21	17.73	28.07	22.51	14.03	9.25	5.85	17.08
		Glister	17.32	19.77	18.84	23.12	19.10	11.68	8.84	3.86	15.32
		Forgetting	20.04	23.83	19.38	28.88	23.77	12.13	12.06	5.54	18.20
		DATM	39.68	40.32	**36.12**	**43.14**	38.35	**35.10**	12.41	9.02	31.76
		PAD	**41.02**	**40.88**	36.08	42.96	**38.64**	35.02	**13.17**	**9.68**	**32.18**
		↑	+26.02	+16.67	+18.35	+14.89	+16.13	+20.99	+3.92	+3.83	+15.10

Table 2: Cross-architecture evaluation of distilled data on unseen networks. Results worse than random selection are indicated with red color. ↑ denotes the performance improvement brought by our method compared with random selection. Tiny denotes Tiny ImageNet.

Method	ConvNet	ResNet18	VGG	AlexNet
Random	33.46	31.95	32.18	26.65
FTD	48.90	46.65	43.24	42.20
DATM	55.03	51.71	**45.38**	45.74
PAD	**55.91**	**52.35**	44.97	**45.92**

(a) Datasets distilled by PAD generalize well across various architectures.

FIEX	FIEM	Accuracy(%)
		66.7
	✓	66.9
✓		67.2
✓	✓	67.4

(b) Each module brings non-trivial improvements.

IR	AEE		
	20	40	60
50%	66.23	66.07	65.92
75%	**67.36**	**67.34**	**66.58**
80%	67.26	67.08	66.47

(c) Set IR as 75% always perform best.

Table 3: **(a)** Cross-Architecture evaluation on CIFAR-100 IPC50. **(b)** Ablation studies on the modules of our method on CIFAR-10 IPC10. **(c)** Results of different sets of data selection hyper-parameters on CIFAR-10 IPC10.

information strategy becomes increasingly effective as IPC increases. More comparisons can be found in Appendix A.3

Cross Architecture Generalization We evaluate the generalizability of our distilled data in both low and high IPC cases. As results reported in Table 3(a), when IPC is small, our distilled data outperforms the previous SOTA method DATM on ResNet and AlexNet while maintaining comparable accuracy on VGG. This suggests that our distilled data on high compressing ratios generalizes well across various unseen networks. Moreover, as reflected in Table 2, our distilled datasets on large IPCs also have the best performance on most evaluated architectures, showing good generalizability in the low compressing ratio case.

4.3 Ablation Study

To validate the effectiveness of each component of our method, we conducted ablation experiments on modules (section 4.3.1) and their hyper-parameter settings (section 4.3.2 and section 4.3.2).

4.3.1 Modules

Our method incorporates two separate modules to filter information extraction (FIEX) and information embedding (FIEM), respectively. To verify their isolated effectiveness, we conduct an ablation study by applying two modules individually. As depicted in Table 3(b), both FIEX and FIEM bring improvements, implying their efficacy. By applying these two modules, we are able to effectively remove unaligned information, improving the distillation performance. More ablation results can be found in Table 8(b).

6

Method	IPC		
	1	10	500
Loss	45.74	66.45	83.47
Uncertainty [4]	46.22	66.99	84.22
EL2N [35]	**47.23**	**67.38**	**84.63**

IPC	Ratio			
	100%	75%	50%	25%
1	**47.2**	46.56	45.98	41.32
10	67.2	**67.34**	66.86	65.15
500	83.71	83.82	**84.23**	**84.64**

Strategy	IPC	
	10	50
Baseline	67.2	76.5
Loss	67.3	77.0
Depth	**67.7**	**77.3**

(a) Using EL2N to measure the difficulty of samples has the best performance.

(b) As IPC increases, removing more shallow-layer parameters becomes more effective.

(c) Using layer depth to select parameters outperforms using matching loss.

Table 4: **(a)** Ablation of different difficulty scoring functions on CIFAR-10. **(b)** Results of masking out different ratios of shallow-layer parameters across various IPCs on CIFAR-10. **(c)** Ablation on the strategy used for parameter selection on CIFAR-10

IPC	PAD	BLiP
1	46.8 (**+0.6**, 80%)	46.3 (+0.2, 80%)
10	66.5 (**+1.1**, 90%)	65.7 (+0.4, 90%)
50	73.0 (**+1.4**, 95%)	72.0 (+0.4, 95%)

IPC	25%	50%	75%	baseline
1	44.1	43.2	41.8	46.9
10	62.2	57.7	51.1	66.9
50	69.2	66.5	58.3	76.1

IPC	SRe^2L	SRe^2L + **PAD(FIEX)**
1	25.4	**26.7** (↑ 1.3)
10	28.2	**29.3** (↑ 1.1)
50	57.2	**57.9** (↑ 0.7)

(a) Data selection (FIEX) in PAD is more effective in improving trajectory matching.

(b) Dicarding deep-layer parameters significantly harms the performance.

(c) PAD can also be applied to SRe^2L and brings non-trivial improvements.

Table 5: (a) We compare our data selection strategy with that of BLiP on CIFAR10. The left in the bracket denotes the improvement over MTT, and the right denotes the percentage of real data used for distillation. (b) Ablation results of discarding deep-layer parameters during information embedding on CIFAR-10. (c) Results of SRe^2L on CIFAR-100 after applying PAD.

4.3.2 Hyper-parameters of Filtering Information Extraction

Initial Ratio and Data Addition Epoch To filter the information learned by agent models, we initialize the training set with only easy samples, and the size is determined by a certain ratio of the total size. Then, we gradually add hard samples into the training set. In practice, we use two hyper-parameters to control the addition process: the initial ratio (IR) of training data for training set initialization and the end epoch of hard sample addition (AEE). These two parameters together control the amount of data agent models can see at each epoch and the speed of adding hard samples.

In Table 3(c), we show the distillation results where different hyper-parameters are utilized. In general, a larger initial ratio and faster speed of addition bring better performances. Although the distillation benefited more from learning simpler information when IPC is small [11], our findings indicate that excessively removing difficult samples (e.g., more than a quarter) early in the training phase can adversely affect the distilled data. This negative impact is likely due to the excessive removal leading to distorted feature distributions within each category. On the other hand, reasonably improving the speed of adding hard samples allows the agent model to achieve a more balanced learning of information of varying difficulty across different stages.

Other Difficulty Scoring Functions Identifying the difficulty of data points is the key to filtering out misaligned information in the extraction step. Here, we compare the effect of using other difficulty-scoring functions to evaluate the difficulty of data. (1) prediction loss of a pre-trained ResNet. (2) uncertainty score [4]. (3) EL2N [35]. As can be observed in Table 4(a), EL2N performs the best across various IPCs; thus, we use it to measure how hard each data point is as default in our method. Note that this can also be replaced with a more advanced data selection algorithm.

4.3.3 Ratios of Parameter Selection

It is important to find a good balance between the percentage of shallow-layer parameters removed from matching and the loss of information. In Table 4(b), we show results obtained on different IPCs by discarding various ratios of shallow-layer parameters. The impact of removing varying proportions of shallow parameters on the distilled data and its relationship with changes in IPC is consistent with prior conclusions. For small IPCs, distilled data requires more low-level basic information. Thus, removing too many shallow-layer parameters causes a negative effect on the

(a) with 100% parameters　　　　　(b) with 75% parameters　　　　　(c) with 50% parameters
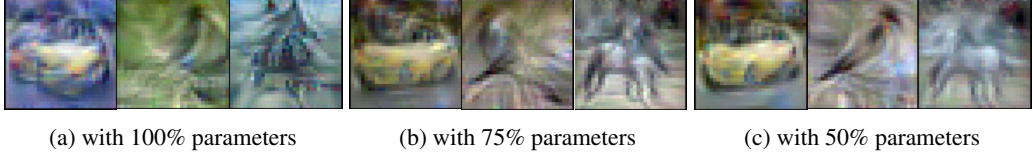
Figure 4: Synthetic images of CIFAR-10 IPC50 obtained by PAD with different ratios of parameter selection. Smoother image features indicate that by removing some shallow-layer parameters during matching, PAD successfully filters out coarse-grained low-level information.

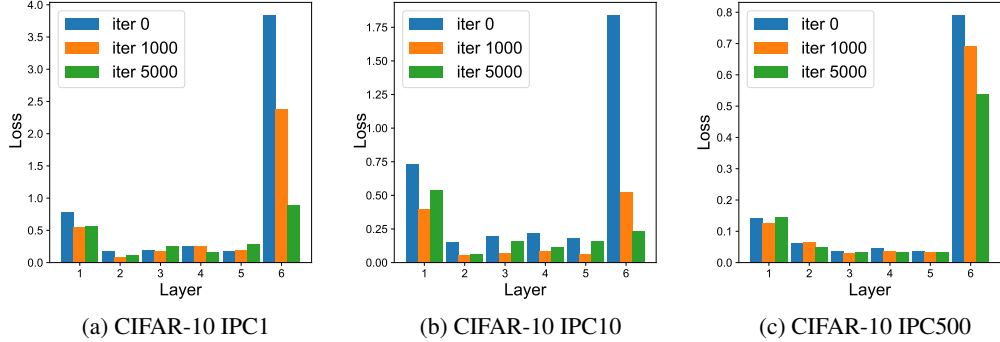(a) CIFAR-10 IPC1　　　　　　　(b) CIFAR-10 IPC10　　　　　　　(c) CIFAR-10 IPC500

Figure 5: Losses of different layers of ConvNet after matching trajectories for 0, 1000, and 5000 iterations. We notice a similar phenomenon on both small (IPC1 and IPC10) and large IPCs (IPC500): losses of shallow-layer parameters fluctuate along the matching process, while losses of deep-layer parameters show a clear trend of decreasing.

classification performance. By contrast, high-level semantic information is more important when it comes to large IPCs. With increasing ratios of shallow-layer parameters being discarded, we can ensure that low-level information is effectively filtered out from the distilled data.

5 Discussion

5.1 Distilled Images with Filtering Information Embedding

To see the concrete patterns brought by removing shallow-layer parameters to perform the trajectory matching, we present distilled images obtained by discarding various ratios of shallow-layer parameters in Figure 4. As can be observed in Figure 4(a), without removing any shallow-layer parameters to filter misaligned information, synthetic images are interspersed with substantial noises. These noises often take the form of coarse and generic information, such as the overall color distribution and edges in the image, which provides minimal utility for precise classification.

By contrast, images distilled by our enhanced methodology (see Figure 4(b) and Figure 4(c)), which includes meticulous masking out shallow-layer parameters during trajectory matching according to the compressing ratio, contain more fine-grained and smoother features. These images also encapsulate a broader range of semantic information, which is crucial for helping the model make accurate classifications. Moreover, we observe a clear trend: as the amount of the removed shallow-layer parameters increases, the distilled images exhibit clearer and smoother features.

5.2 Rationale for Parameter Selection

In this section, we analyze from the perspective of trajectory matching why shallow-layer parameters should be masked out. In Figure 5, we present the changes in trajectory matching loss across different layers as the distillation progresses. Compared to the deep-layer parameters of the agent model, a substantial number of shallow-layer parameters exhibit low loss values that fluctuate during the matching process (see Figure 5). By contrast, the loss values of the deep layers are much higher but

(a) Match shallow layers only   (b) Original   (c) Match deep layers only
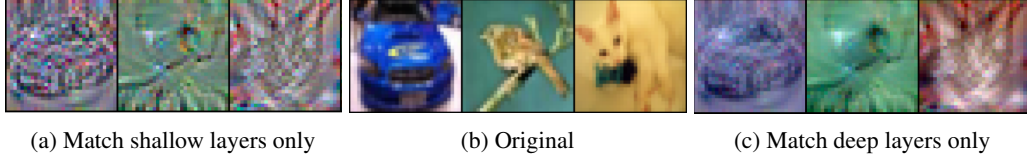
Figure 6: Synthetic images visualization with parameter selection. Matching parameters in shallow layers produces an abundance of low-level texture features, whereas patterns generated by matching deep-layer parameters embody richer high-level semantic information.

consistently decrease as distillation continues. This suggests that matching shallow layers primarily conveys low-level information that is readily captured by the synthetic data and quickly saturated. Consequently, the excessive addition of such low-level information produces noise, reducing the quality of distilled datasets.

For a concrete visualization, we provide distilled images resulting from using only shallow-layer parameters or only deep-layer parameters to match trajectories in Figure 6. The coarse image features depicted in Figure 6(a) further substantiate our analysis.

To further demonstrate the importance of deep-layer parameters, we show performances of discarding deep-layer parameters in Table 5(b). As can be observed, there are significant performance drops when these parameters are not used for distillation. As the discarding ratio increases, the performance drop becomes more serious for all IPCs. Also, the impact of discarding deep-layer parameters is more significant on larger IPCs. These results verify that deep-layer parameters are more important than shallow-layer parameters.

5.3 Parameter Selection Strategy

In the previous section, we observed a positive correlation between the depth of the model layers and the magnitude of their trajectory-matching losses. Notably, the loss in the first layer of the ConvNet was higher compared to other shallow layers. Consequently, we further compared different parameter alignment strategies, specifically by sorting the parameters based on their matching losses and excluding a certain proportion of parameters with lower losses. Higher loss values indicate greater discrepancies in parameter weights; thus, continuing to match these parameters can inject more information into the synthetic data. As shown in Table 4(c), sorting by loss results in an improvement compared with no parameter alignment, but filtering based on parameter depth proves to be more effective.

5.4 Other Methods with Data Selection

To further demonstrate the effectiveness of our FIEX, we compare ours with BLiP [48], which also uses a data selection strategy before distillation. It proposes a data utility indicator to evaluate if samples are 'useful' given an IPC setting, and then samples with low utility are pruned. As shown in Table 5(a), PAD brings better performance improvements on IPC1/10/50. Under a given data-dropping ratio, PAD's improvements over BLiP get larger as the IPC increases. This supports our conclusion that difficulty misalignment between IPCs and real data used is more harmful. PAD's data selection module is more effective in removing such misaligned information.

5.5 Generalization to Other Methods

In Section 2, we show that the two filtering modules of PAD can be applied on seminal matching-based DD baselines (DC, DM, MTT) and improve their performances remarkably. To catch up with the latest DD progress, we combine PAD with a more recent DD method that achieves great success on high-resolution datasets, SRe^2L [49], to show that PAD can also generalize well on other methods. As shown in Table c, by filtering out misaligned information extracted in SRe^2L's *squeeze* and *recover* stages, the performance of SRe^2L improves on both small and large IPC settings. Particularly, PAD's information extraction filter brings more pronounced improvements to smaller IPCs This further validates PAD's efficacy in aligning information of dataset distillation and demonstrates that

PAD also has decent generalizability on other methods that involve an information-extraction-like or information-embedding-like component.

6 Related Work

Introduced by [47], dataset distillation aims to synthesize a compact set of data that allows models to achieve similar test performances compared with the original dataset. Since then, a number of studies have explored various approaches. These methods can be divided into three types: kernel-based, matching-based, and using generative models [51].

Kernel-based methods are able to achieve closed-form solutions for the inner optimization [33] via kernel ridge regression with NTK [23]. FRePo [56] distills a compact dataset through neural feature regression and reduces the training cost.

Matching-based methods first use agent models to extract information from the target dataset by recording a specific metric [8, 24, 26, 40]. Representative works that design different metrics include DC [55] that matches gradients, DM [54] that matches distributions, and MTT [1] that matches training trajectories. Then, the distilled dataset is optimized by minimizing the matched distance between the metric computed on synthetic data and the record one from the previous step. Following this workflow, many works have been proposed to improve the efficacy of the distilled dataset.

For example, CAFE [46] preserves the real feature distribution and the discriminative power of the synthetic data and achieves prominent generalization ability across various architectures. DREAM [27] employs K-Means to select representative samples for distillation and improves the distillation efficiency. DATM [11] proposes to match early trajectories for small IPCs and late trajectories for large IPCs, achieving SOTA performances on several benchmarks. BLiP [48] and Prune-then-Distill [44] discover the issue of data redundancy in the previous distillation framework and propose to prune the real dataset before distillation. PDD [3] identifies the change of learned pattern complexity at different training stages and proposes a multi-stage distillation process where each synthetic subset is conditioned on the previous ones to alleviate the above challenge. Moreover, new metrics such as spatial attention maps [16, 38] have also been introduced and achieved promising performance in distilling large-scale datasets.

Generative methods such as GANs [9, 14, 15, 45] and diffusion models [10, 32, 36] can also be used to distill high quality datasets. DiM [45] uses deep generative models to store information of the target dataset. GLaD [2] transfers synthetic data optimization from the pixel space to the latent space by employing deep generative priors. It enhances the generalizability of previous methods.

Other methods RDED [43] proposes a computationally efficient DD method that doesn't require synthetic image optimization by extracting and rearranging key image patches. SRe^2L [49] introduces a "squeeze, recover, relabel" procedure that decouples previous bi-level optimization and achieves success on high-resolution settings with lower computational costs.

7 Conclusion

In this work, we find a limitation of existing Dataset Distillation methods in that they will introduce misaligned information to the distilled datasets. To alleviate this, we propose PAD, which incorporates two modules to filter out misaligned information. For information extraction, PAD prunes the target dataset based on sample difficulty for different IPCs so that only information with aligned difficulty is extracted by the agent model. For information embedding, PAD discards part of shallow-layer parameters to avoid injecting low-level basic information into the synthetic data. PAD achieves SOTA performance on various benchmarks. Moreover, we show PAD can also be applied to methods based on matching gradients and distributions, bringing improvements across various IPC settings.

Limitations   Our alignment strategy could also be applied to methods based on matching gradients and distributions. However, due to the limitation of computing resources, for methods based on matching distributions and gradients, we have only validated our method's effectiveness on DM [54] and DC [55], and SRe^2L [49] (see Table 5(c), Table 6 and Table 7).

References

[1] George Cazenavette, Tongzhou Wang, Antonio Torralba, Alexei A. Efros, and Jun-Yan Zhu. Dataset distillation by matching training trajectories. *2022 IEEE/CVF Conference on Computer Vision and Pattern Recognition (CVPR)*, pages 10708–10717, 2022.

[2] George Cazenavette, Tongzhou Wang, Antonio Torralba, Alexei A. Efros, and Jun-Yan Zhu. Generalizing dataset distillation via deep generative prior. *2023 IEEE/CVF Conference on Computer Vision and Pattern Recognition (CVPR)*, pages 3739–3748, 2023.

[3] Xuxi Chen, Yu Yang, Zhangyang Wang, and Baharan Mirzasoleiman. Data distillation can be like vodka: Distilling more times for better quality. *ArXiv*, abs/2310.06982, 2023.

[4] Cody Coleman, Christopher Yeh, Stephen Mussmann, Baharan Mirzasoleiman, Peter Bailis, Percy Liang, Jure Leskovec, and Matei Zaharia. Selection via proxy: Efficient data selection for deep learning. *arXiv preprint arXiv:1906.11829*, 2019.

[5] Justin Cui, Ruochen Wang, Si Si, and Cho-Jui Hsieh. Scaling up dataset distillation to imagenet-1k with constant memory. In *International Conference on Machine Learning*, 2022.

[6] Tian Dong, Bo Zhao, and Lingjuan Lyu. Privacy for free: How does dataset condensation help privacy? *ArXiv*, abs/2206.00240, 2022.

[7] Jiawei Du, Yiding Jiang, Vincent Y. F. Tan, Joey Tianyi Zhou, and Haizhou Li. Minimizing the accumulated trajectory error to improve dataset distillation. *2023 IEEE/CVF Conference on Computer Vision and Pattern Recognition (CVPR)*, pages 3749–3758, 2022.

[8] Jiawei Du, Qin Shi, and Joey Tianyi Zhou. Sequential subset matching for dataset distillation. *ArXiv*, abs/2311.01570, 2023.

[9] Ian J. Goodfellow, Jean Pouget-Abadie, Mehdi Mirza, Bing Xu, David Warde-Farley, Sherjil Ozair, Aaron C. Courville, and Yoshua Bengio. Generative adversarial networks. *Communications of the ACM*, 63:139 – 144, 2014.

[10] Jianyang Gu, Saeed Vahidian, Vyacheslav Kungurtsev, Haonan Wang, Wei Jiang, Yang You, and Yiran Chen. Efficient dataset distillation via minimax diffusion. *ArXiv*, abs/2311.15529, 2023.

[11] Ziyao Guo, Kai Wang, George Cazenavette, Hui Li, Kaipeng Zhang, and Yang You. Towards lossless dataset distillation via difficulty-aligned trajectory matching. *ArXiv*, abs/2310.05773, 2023.

[12] Kaiming He, X. Zhang, Shaoqing Ren, and Jian Sun. Deep residual learning for image recognition. *2016 IEEE Conference on Computer Vision and Pattern Recognition (CVPR)*, pages 770–778, 2015.

[13] Haifeng Jin, Qingquan Song, and Xia Hu. Auto-keras: An efficient neural architecture search system. *Proceedings of the 25th ACM SIGKDD International Conference on Knowledge Discovery & Data Mining*, 2018.

[14] Tero Karras, Samuli Laine, and Timo Aila. A style-based generator architecture for generative adversarial networks. *2019 IEEE/CVF Conference on Computer Vision and Pattern Recognition (CVPR)*, pages 4396–4405, 2018.

[15] Tero Karras, Samuli Laine, Miika Aittala, Janne Hellsten, Jaakko Lehtinen, and Timo Aila. Analyzing and improving the image quality of stylegan. *2020 IEEE/CVF Conference on Computer Vision and Pattern Recognition (CVPR)*, pages 8107–8116, 2019.

[16] Samir Khaki, Ahmad Sajedi, Kai Wang, Lucy Z. Liu, Yuri A. Lawryshyn, and Konstantinos N. Plataniotis. Atom: Attention mixer for efficient dataset distillation, 2024.

[17] Krishnateja Killamsetty, Durga Sivasubramanian, Ganesh Ramakrishnan, Abir De, and Rishabh K. Iyer. Grad-match: Gradient matching based data subset selection for efficient deep model training. In *International Conference on Machine Learning*, 2021.

[18] Krishnateja Killamsetty, Durga Sivasubramanian, Ganesh Ramakrishnan, Rishabh Iyer University of Texas at Dallas, Indian Institute of Technology Bombay Institution One, and IN Two. Glister: Generalization based data subset selection for efficient and robust learning. In *AAAI Conference on Artificial Intelligence*, 2020.

[19] Alex Krizhevsky. Learning multiple layers of features from tiny images. 2009.

[20] Alex Krizhevsky, Ilya Sutskever, and Geoffrey E. Hinton. Imagenet classification with deep convolutional neural networks. *Communications of the ACM*, 60:84 – 90, 2012.

[21] Ya Le and Xuan S. Yang. Tiny imagenet visual recognition challenge. 2015.

[22] Yann LeCun, Léon Bottou, Yoshua Bengio, and Patrick Haffner. Gradient-based learning applied to document recognition. *Proc. IEEE*, 86:2278–2324, 1998.

[23] Jaehoon Lee, Lechao Xiao, Samuel S. Schoenholz, Yasaman Bahri, Roman Novak, Jascha Narain Sohl-Dickstein, and Jeffrey Pennington. Wide neural networks of any depth evolve as linear models under gradient descent. *Journal of Statistical Mechanics: Theory and Experiment*, 2020, 2019.

[24] Saehyung Lee, Sanghyuk Chun, Sangwon Jung, Sangdoo Yun, and Sung-Hoon Yoon. Dataset condensation with contrastive signals. In *International Conference on Machine Learning*, 2022.

[25] Dai Liu, Jindong Gu, Hu Cao, Carsten Trinitis, and Martin Schulz. Dataset distillation by automatic training trajectories. *ArXiv*, abs/2407.14245, 2024.

[26] Haoyang Liu, Tiancheng Xing, Luwei Li, Vibhu Dalal, Jingrui He, and Haohan Wang. Dataset distillation via the wasserstein metric. *ArXiv*, abs/2311.18531, 2023.

[27] Yanqing Liu, Jianyang Gu, Kai Wang, Zheng Hua Zhu, Wei Jiang, and Yang You. Dream: Efficient dataset distillation by representative matching. *2023 IEEE/CVF International Conference on Computer Vision (ICCV)*, pages 17268–17278, 2023.

[28] Noel Loo, Ramin M. Hasani, Mathias Lechner, and Daniela Rus. Dataset distillation with convexified implicit gradients. *ArXiv*, abs/2302.06755, 2023.

[29] Aravindh Mahendran and Andrea Vedaldi. Visualizing deep convolutional neural networks using natural pre-images. *International Journal of Computer Vision*, 120:233 – 255, 2016.

[30] Wojciech Masarczyk and Ivona Tautkute. Reducing catastrophic forgetting with learning on synthetic data. In *CVPR Workshop*, 2020.

[31] Baharan Mirzasoleiman, Jeff A. Bilmes, and Jure Leskovec. Coresets for data-efficient training of machine learning models. In *International Conference on Machine Learning*, 2019.

[32] Brian B. Moser, Federico Raue, Sebastián M. Palacio, Stanislav Frolov, and Andreas Dengel. Latent dataset distillation with diffusion models. *ArXiv*, abs/2403.03881, 2024.

[33] Timothy Nguyen, Zhourung Chen, and Jaehoon Lee. Dataset meta-learning from kernel ridge-regression. *ArXiv*, abs/2011.00050, 2020.

[34] Ramakanth Pasunuru and Mohit Bansal. Continual and multi-task architecture search. *ArXiv*, abs/1906.05226, 2019.

[35] Mansheej Paul, Surya Ganguli, and Gintare Karolina Dziugaite. Deep learning on a data diet: Finding important examples early in training. In *Neural Information Processing Systems*, 2021.

[36] Robin Rombach, A. Blattmann, Dominik Lorenz, Patrick Esser, and Björn Ommer. High-resolution image synthesis with latent diffusion models. *2022 IEEE/CVF Conference on Computer Vision and Pattern Recognition (CVPR)*, pages 10674–10685, 2021.

[37] Andrea Rosasco, Antonio Carta, Andrea Cossu, Vincenzo Lomonaco, and Davide Bacciu. Distilled replay: Overcoming forgetting through synthetic samples. In *International Workshop on Continual Semi-Supervised Learning*, 2021.

[38] Ahmad Sajedi, Samir Khaki, Ehsan Amjadian, Lucy Z. Liu, Yuri A. Lawryshyn, and Konstantinos N. Plataniotis. Datadam: Efficient dataset distillation with attention matching. In *Proceedings of the IEEE/CVF International Conference on Computer Vision (ICCV)*, pages 17097–17107, October 2023.

[39] Ramprasaath R. Selvaraju, Abhishek Das, Ramakrishna Vedantam, Michael Cogswell, Devi Parikh, and Dhruv Batra. Grad-cam: Visual explanations from deep networks via gradient-based localization. *International Journal of Computer Vision*, 128:336 – 359, 2016.

[40] Seung-Jae Shin, Heesun Bae, DongHyeok Shin, Weonyoung Joo, and Il-Chul Moon. Loss-curvature matching for dataset selection and condensation. In *International Conference on Artificial Intelligence and Statistics*, 2023.

[41] Karen Simonyan and Andrew Zisserman. Very deep convolutional networks for large-scale image recognition. *CoRR*, abs/1409.1556, 2014.

[42] Ben Sorscher, Robert Geirhos, Shashank Shekhar, Surya Ganguli, and Ari Morcos. Beyond neural scaling laws: beating power law scaling via data pruning. *Advances in Neural Information Processing Systems*, 35:19523–19536, 2022.

[43] Peng Sun, Bei Shi, Daiwei Yu, and Tao Lin. On the diversity and realism of distilled dataset: An efficient dataset distillation paradigm. *ArXiv*, abs/2312.03526, 2023.

[44] Anirudh S. Sundar, Gökçe Keskin, Chander Chandak, I-Fan Chen, Pegah Ghahremani, and Shalini Ghosh. Prune then distill: Dataset distillation with importance sampling. *ICASSP 2023 - 2023 IEEE International Conference on Acoustics, Speech and Signal Processing (ICASSP)*, pages 1–5, 2023.

[45] Kai Wang, Jianyang Gu, Daquan Zhou, Zheng Hua Zhu, Wei Jiang, and Yang You. Dim: Distilling dataset into generative model. *ArXiv*, abs/2303.04707, 2023.

[46] Kai Wang, Bo Zhao, Xiangyu Peng, Zheng Hua Zhu, Shuo Yang, Shuo Wang, Guan Huang, Hakan Bilen, Xinchao Wang, and Yang You. Cafe learning to condense dataset by aligning features. 2022.

[47] Tongzhou Wang, Jun-Yan Zhu, Antonio Torralba, and Alexei A. Efros. Dataset distillation, 2020.

[48] Yue Xu, Yong-Lu Li, Kaitong Cui, Ziyu Wang, Cewu Lu, Yu-Wing Tai, and Chi-Keung Tang. Distill gold from massive ores: Efficient dataset distillation via critical samples selection. *ArXiv*, abs/2305.18381, 2023.

[49] Zeyuan Yin, Eric P. Xing, and Zhiqiang Shen. Squeeze, recover and relabel: Dataset condensation at imagenet scale from a new perspective. *ArXiv*, abs/2306.13092, 2023.

[50] Qiying Yu, Yang Liu, Yimu Wang, Ke Xu, and Jingjing Liu. Multimodal federated learning via contrastive representation ensemble. *ArXiv*, abs/2302.08888, 2023.

[51] Ruonan Yu, Songhua Liu, and Xinchao Wang. Dataset distillation: A comprehensive review. *IEEE Transactions on Pattern Analysis and Machine Intelligence*, 46:150–170, 2023.

[52] Bo Zhao and Hakan Bilen. Dataset condensation with differentiable siamese augmentation. In *International Conference on Machine Learning*, 2021.

[53] Bo Zhao and Hakan Bilen. Dataset condensation with differentiable siamese augmentation. In *International Conference on Machine Learning*, 2021.

[54] Bo Zhao and Hakan Bilen. Dataset condensation with distribution matching. *2023 IEEE/CVF Winter Conference on Applications of Computer Vision (WACV)*, pages 6503–6512, 2021.

[55] Bo Zhao, Konda Reddy Mopuri, and Hakan Bilen. Dataset condensation with gradient matching. *ArXiv*, abs/2006.05929, 2020.

[56] Yongchao Zhou, Ehsan Nezhadarya, and Jimmy Ba. Dataset distillation using neural feature regression. *ArXiv*, abs/2206.00719, 2022.

IPC	Ratio							Baseline
	5%	10%	15%	20%	25%	30%	50%	
1	28.0	28.4	28.5	**29.1**	28.8	28.1	27.9	27.8
10	45.2	45.5	45.7	46.1	**46.3**	45.3	44.5	44.7
500	71.7	**71.9**	71.2	71.4	70.3	69.8	67.1	71.4

(a) Removing various ratios of hard/easy samples improves DC on small/large IPCs.

IPC	Ratio							Baseline
	5%	10%	15%	20%	25%	30%	50%	
1	26.8	27.1	27.3	27.9	28.2	28.5	**29.2**	26.4
10	48.6	48.9	49.7	**50.3**	49.6	49.2	48.5	48.4
500	75.6	76.2	**76.3**	75.8	75.3	74.6	74.2	75.1

(b) Removing various ratios of hard/easy samples improves DM on small/large IPCs.

Table 6: Results of filtering information extraction by removing hard/easy samples in DC(a) and DM(b) on CIFAR-10.

Appendix

A   Additional Experimental Results and Findings

A.1   Filtering Misaligned Information in DC and DM

Although PAD is implemented based on trajectory matching methods, we also test our proposed data alignment and parameter alignment on gradient matching and distribution matching. The performances of enhanced DC and DM with each of the two modules are reported in Table 6 and Tabl 7, respectively. We provide details of how we integrate these two modules into gradient matching and distribution matching in the following sections.

Gradient Matching We use the official implementation[3] of DC [55]. In the Information Extraction step, DC uses an agent model to calculate the gradients after being trained on the target dataset. We employ filter misaligned information in this step as follows: When IPC is small, a certain ratio of hard samples is removed from the target dataset so that the recorded gradients only contain simple information. Conversely, when IPC becomes large, we remove easy samples instead.

In the Information Embedding step, DC optimizes the synthetic data by back-propagating on the gradient matching loss. The loss is computed by summing the differences in gradients between each pair of model parameters. Thus, we apply parameter selection by discarding a certain ratio of parameters in the shallow layers.

Distribution Matching We use the official implementation of DM [54], which can be accessed via the same link as DC. In the Information Extraction step, DM uses an agent model to generate embeddings of input images from the target dataset. Similarly, filtering information extraction is applied by removing hard samples for small IPCs and easy samples for large IPCs.

In the Information Embedding step, since DM only uses the output of the last layer to match distributions, we modify the implementation of the network such that outputs of each layer in the model are returned by the forward function. Then, we perform parameter selection following the same practice as before.

A.2   Data Scheduler

To support the way we design the data scheduler to remove easy samples at late trajectories directly, we compare direct removal with gradual removal. The implementation of gradual removal is similar to the hard sample addition. Experimental results are shown in Table 8(a) on CIFAR-10 and CIFAR-100. Only large IPCs are tested because only large IPCs match late trajectories. As can be observed, compared with gradually removing easy data, deleting easy samples in one operation performs better. This supports our conclusion that after being trained on the full dataset for some epochs, it is

---

[3]https://github.com/VICO-UoE/DatasetCondensation.git

IPC	Ratio			Baseline
	25%	50%	75%	
10	**45.2**	44.7	43.8	44.9
500	72.5	72.8	**73.4**	72.2

IPC	Ratio			Baseline
	25%	50%	75%	
10	**49.5**	49.1	48.3	48.9
500	75.5	75.9	**76.3**	75.1

(a) Matching gradients from deep-layer parameters leads to improvements.

(b) Matching distributions from deep-layer parameters leads to improvements.

Table 7: Results of filtering information embedding by masking out shallow-layer parameters for metric computation in DC(a) and DM(b) on CIFAR-10.

Strategy	CIFAR-10 IPC		CIFAR-100 IPC	
	50	100	50	100
Gradually remove	84.2	86.4	55.6	58.3
Directly remove	**84.6**	**86.7**	**55.9**	**58.5**

FIEX	FIEM	Accuracy(%)
		55.0
	✓	55.5
✓		55.8
✓	✓	56.2

(a) Directly removing easy samples at late trajectories brings better performances.

(b) Each module brings non-trivial improvements to the baseline.

Table 8: (a) Comparison between gradually removing easy samples and directly removing easy samples during trajectory training. (b) Ablation results on CIFAR-100 IPC50.

more effective for the model to focus on learning hard information rather than easy information by removing easy samples directly.

A.3 Comparison with Knowledge Distillation Methods

Recently, new advancements, represented by RDED [43], in DD have applied knowledge distillation to evaluate distilled datasets and achieved remarkable performance improvements. Specifically, a randomly initialized student model is trained on synthetic data alongside a teacher model. The objective is to minimize the Kullback-Leibler (KL) divergence between the student model's output and the teacher model's output on the same batch of synthetic data.

To compare with such a method, we adopt its knowledge distillation strategy during evaluation to ensure a fair comparison. Other experimental settings of PAD are the same. As shown in Table 9, PAD demonstrates superior performances in most of the settings, especially when the compressing ratio is higher (larger IPCs). On small IPCs, the knowledge distillation leads to a drop in PAD's pure DD performance (Table 1). This is because knowledge from a well-trained teacher exceeds the capacity of small IPCs.

B Experimental Settings

We use DATM [11] as the backbone TM algorithm, and our proposed PAD is built upon. Thus, our configurations for distillation, evaluation, and network are consistent with DATM.

Distillation. We conduct the distillation process for 10,000 iterations to ensure full convergence of the optimization. By default, ZCA whitening is applied in all the experiments.

Evaluation. We train a randomly initialized network on the distilled dataset and evaluate its performance on the entire validation set of the original dataset. Following DATM [11], the evaluation networks are trained for 1000 epochs to ensure full optimization convergence. For fairness, the experimental results of previous distillation methods in both low and high IPC settings are sourced from [11].

Network. We employ a range of networks to assess the generalizability of our distilled datasets. For scaling ResNet, LeNet, and AlexNet to Tiny-ImageNet, we modify the stride of their initial convolutional layer from 1 to 2. In the case of VGG, we adjust the stride of its final max pooling layer from 1 to 2. The MLP used in our evaluations features a single hidden layer with 128 units.

Dataset	CIFAR10			CIFAR-100			TinyImageNet		
IPC	1	50	500	1	10	50	1	10	50
RDED	23.5±0.3	50.2±0.3	87.2±0.5	**19.6±0.3**	48.1±0.3	57.0±0.1	**12.0±0.1**	**39.6±0.1**	47.6±0.2
PAD	**26.8±0.6**	**62.3±0.5**	**89.6±0.3**	16.4±0.4	**50.2±0.3**	**59.3±.2**	10.1±0.3	37.2±0.5	**48.5±0.3**

Table 9: Comparison between PAD and RDED on CIFAR-10, CIFAR-100, and TinyImageNet. PAD achieves superior performances in 6 out of 9 settings. On larger IPCs, PAD's advantage is more pronounced.

Hyper-parameters. Hyper-parameters of our experiments on CIFAR-10, CIFAR-100, and TinyImageNet are reported in Table 10. Hyper-parameters can be divided into three parts, including FIEX, FIEM, and trajectory matching (TM). For FIEX, the ratio of easy samples removed for all IPCs is 10%. Soft labels are applied in all experiments, we set its momentum to 0.9.

Compute resources. Our experiments are run on 4 NVIDIA A100 GPUs, each with 80 GB of memory. The amount of GPU memory needed is mainly determined by the batch size of synthetic data and the number of steps that the agment model is trained on synthetic data. To reduce the GPU usage when IPC is large, one can apply TESLA [5] or simply reducing the synthetic steps N or the synthetic batch size. However, the decrement of hyper-parameters shown in Table 10 could result in performance degradation.

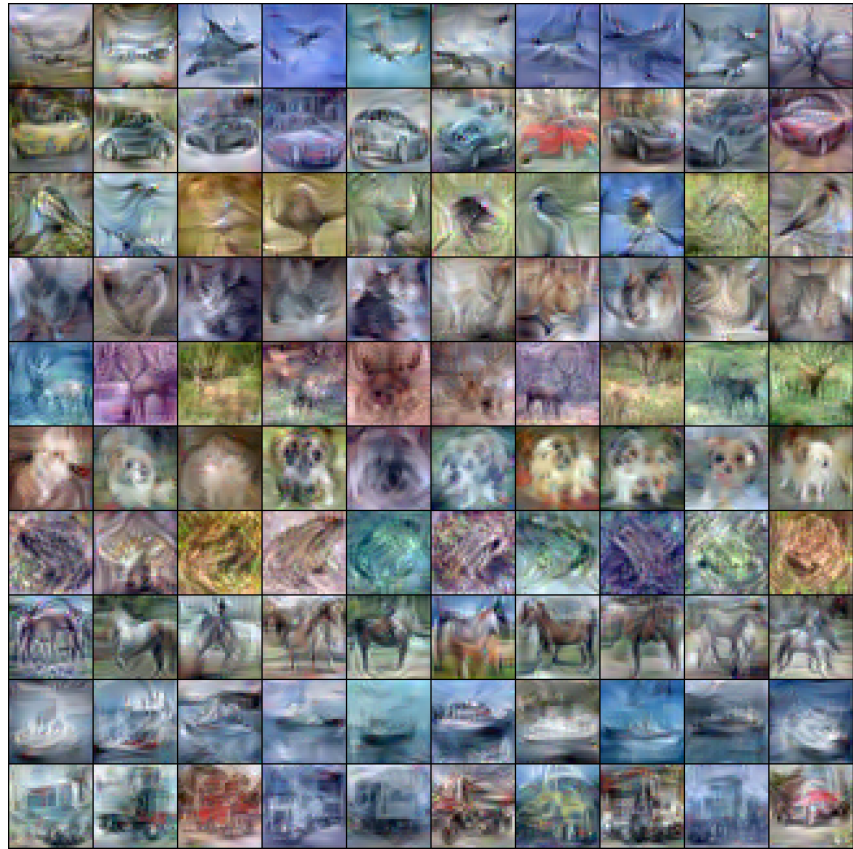| Dataset	IPC	DA		PA							TM		
		IR	AEE	α	N	M	T^-	T	T^+	Interval	Synthetic Batch Size	Learning Rate (Label)	Learning Rate (Pixels)
CIFAR-10	1	0.75	20	0%	80	2	0	4	4	-	10	5	100
	10			25%	80	2	0	10	20	100	100	2	100
	50			25%	80	2	0	20	40	100	500	2	1000
	500			50%	80	2	40	60	60	-	1000	10	50
	1000			75%	80	2	40	60	60	-	1000	10	50
CIFAR-100	1	0.75	40	0%	40	3	0	10	20	100	100	10	1000
	10			25%	80	2	0	20	40	100	1000	10	1000
	50			50%	80	2	40	60	80	100	1000	10	1000
	100			50%	80	2	40	80	80	-	1000	10	50
TI	1	0.75	40	0%	60	2	0	15	30	400	200	10	10000
	10			25%	60	2	0	20	40	100	250	10	100
	50			50%	80	2	20	40	60	100	250	10	100

Table 10: Hyper-parameters for different benchmarks.

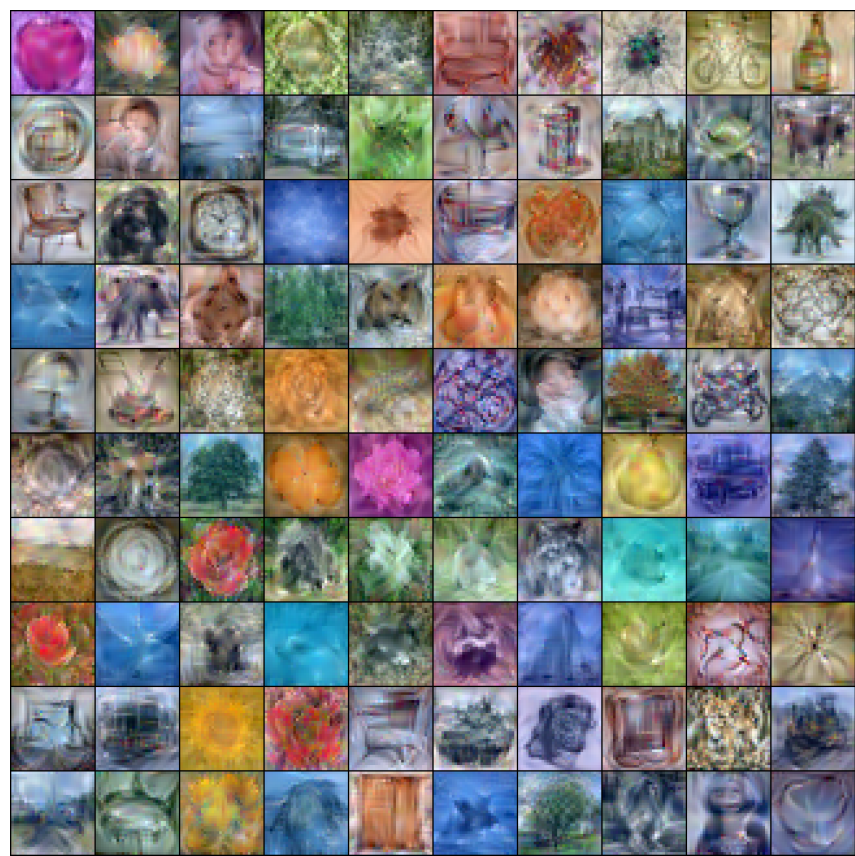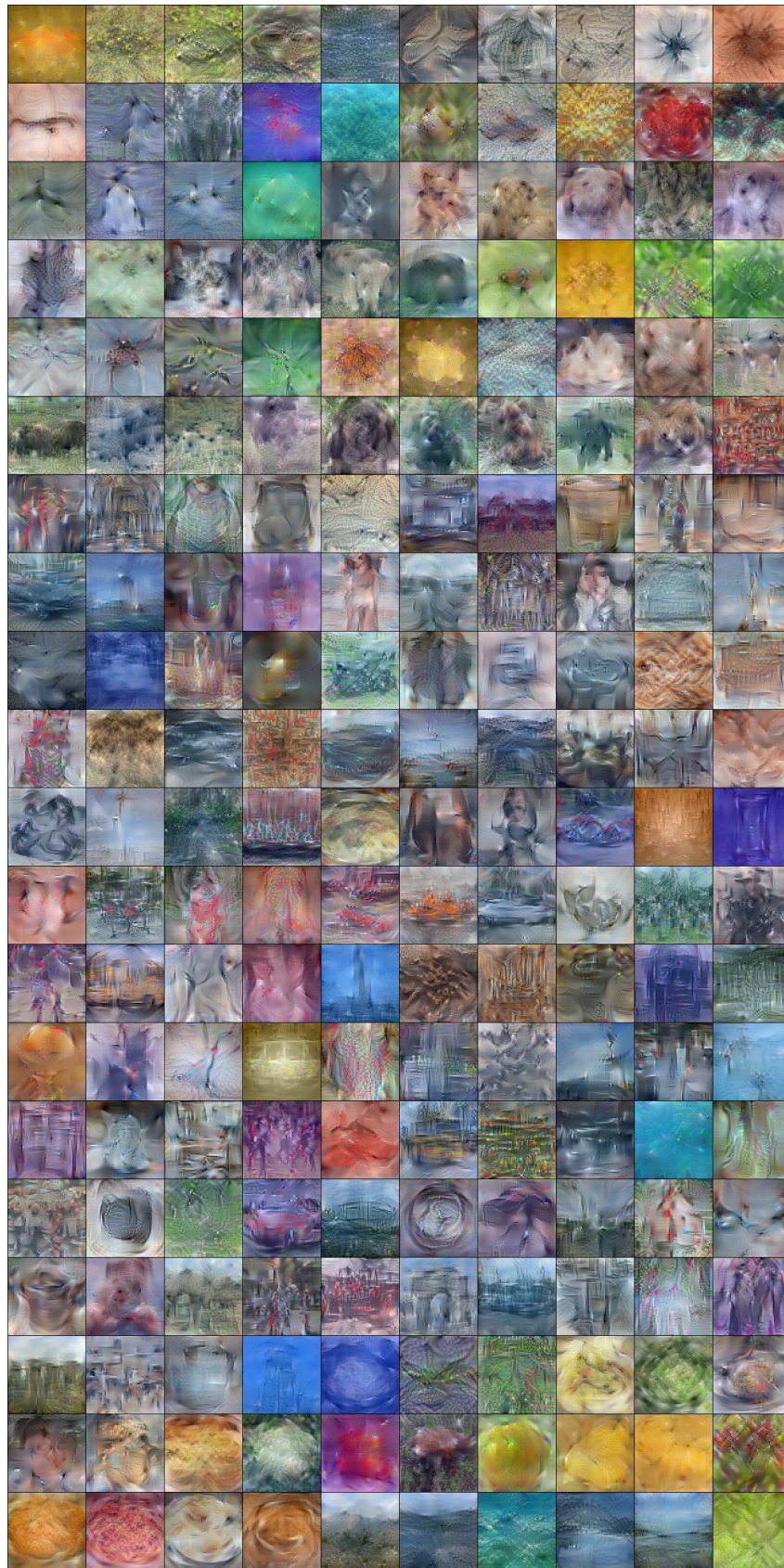Figure 7: Distilled images of CIFAR-10 IPC10

Figure 8: Distilled images of CIFAR-100 IPC1

Figure 9: Distilled images of Tiny-ImageNet IPC1